WILEY-VCH

Title: Towards Stretchable Self-Powered Sensors Based on the Thermoelectric Response of PEDOT:PSS/Polyurethane Blends.

Prospero J. Taroni, Giovanni Santagiuliana, Kening Wan, Philip Calado, Manting Qiu, Han Zhang, Nicola M. Pugno, Matteo Palma, Natalie Stingelin-Stutzman, Martin Heeney, Oliver Fenwick, Mark Baxendale, Emiliano Bilotti*

P.J. Taroni, G. Santagiuliana, K. Wan, Dr. H. Zhang, Dr. O. Fenwick, Dr. E. Bilotti
School of Engineering and Material Sciences, Queen Mary University of London, Mile End Road, E1 4NS, London, UK
E-mail: e.bilotti@qmul.ac.uk
Dr. M. Baxendale, M. Qiu
School of Physics and Astronomy, Queen Mary University of London, Mile End Road, London, E1 4NS, UK
Prof. N. Stingelin-Stutzman
School of Materials Sciences, Georgia Tech, 771 Ferst Drive, J. Erskine Love Building, Atlanta, GA 30332-0245
Prof. M. Heeney,
School of Chemistry and Centre of Plastic Electronics, Imperial College London, London SW7 2AZ, UK
P. Calado,
School of Physics, Imperial College London, London SW7 2AZ, UK
Prof. N. M. Pugno
Laboratory of Bio-inspired & Graphene Nanomechanics, Department of Civil, Environmental and Mechanical Engineering, University of Trento, Via Mesiano 77, 38123 Trento, Italy.
Ket-Lab, Edoardo Amaldi Foundation, Italian Space Agency, Via del Politecnico snc, 00133 Rome, Italy.
Dr M. Palma
School of Biological and Chemical Sciences, Joseph Priestley building, Mile End Road, London, E1 4NS

Abstract:

The development of new flexible and stretchable sensors addresses the demands of upcoming

application fields like internet-of-things, soft robotics and health/structure monitoring.

However, finding a reliable and robust power source to operate these devices, particularly in

off-the-grid, maintenance-free applications, still poses a great challenge. The exploitation of

1

ubiquitous temperature gradients, as the source of energy, could become a practical solution, since the recent discovery of the outstanding thermoelectric properties of a conductive polymer, poly(3,4-ethylenedioxythiophene)-poly(styrenesulfonate) (PEDOT:PSS). Unfortunately the use of PEDOT:PSS is currently constrained by its brittleness and limited processability. Herein, PEDOT:PSS is blended with a commercial elastomeric polyurethane (Lycra®), to obtain tough and processable self-standing films. A remarkable strain-at-break of ~700% is achieved for blends with 90 wt.% Lycra®, after ethylene glycol (EG) treatment, without affecting the Seebeck voltage. We demonstrate for the first time the viability of these novel blends as stretchable self-powered sensors.

1. Introduction

The fast developing field of wearable electronics for autonomous monitoring is combining smart textile technology with state of the art wireless sensing communication, and it could soon experience exponential growth as new applications are being considered for fields such as internet-of-things, soft robotics, medicine, defence, advertising, fashion and many others.[1–5] On the other hand, numerous challenges are still to be overcome, including the need for improved materials that are not only responsive to a specific stimuli but can also conform to the objects monitored, for instance being flexible and stretchable, as well as durable.[6] Another important requirement is to make the sensors autonomous and self-powered, particularly desirable in off-grid, maintenance-free conditions, where battery replacement is not practical, economical or feasible.[5] There have been different research strategies for finding sustainable, small scale energy harvesting systems to recharge batteries or directly power sensor devices, with long lasting and reliable supplies. This has been demosntrated so far using triboelectric,[7–11] photovoltaic,[5,12] piezoelectric,[5,13,14] radiofrequency,[14] thermoelectric (TE) systems,[14–18] and others.[19–21] In the last instance, conventional TE technology has also been considered as a power source for integrated sensors of pressure,[22] corrosion,[23] heat flow,[24] vibration,[25] heart

rate,[26] and other stimuli.[27–31]. The utilization of conjugated polymers as the active component of a TE device is a relatively recent concept,[35,36] but it is rather attractive where flexibility is needed, enabling a new generation of novel, low-cost, low-powered wearable, or even remote, sensors. There are many desirable attributes driving the investigation of polymer TE materials, such as low toxicity, ubiquity and abundance of constitutive elements, as well as ease in processing by various extablished coating or printing techniques. Poly(3,4-ethylenedioxythiophene)-poly(styrenesulfonate) (PEDOT:PSS) is at the centre of the effort to achieve thermoelectric power conversion efficiencies comparable to those of inorganic thermoelectric materials. In 2003, PEDOT was reported to have a dimensionless figure of merit (zT value) as high as 0.42. [37] This result is within close reach from the best commercial inorganic materials used for room temperature applications, such as bismuth telluride compounds, with zT value around 1.[38] Promising results were also obtained by combining PEDOT, or other conductive polymers (e.g. P3HT and PANi), with carbon nanotubes and other nanoparticles. [39-42] PEDOT was further studied as a p-type TE material, [43–53] and shown to be sensitive to stimuli like temperature and pressure.[54] However, a number of challenges still restrict its commercial exploitation, including low toughness and tear resistance, in addition to processing constraints, limited to film casting from water solution, while bulk (greater than tens of microns thick) processing is needed to fulfil current TE device design requirements.

Here we propose a novel strategy for overcoming the above limitations, consisting of blending PEDOT:PSS with a commercial polyurethane (Lycra®), followed by post-treatment of the films with ethylene glycol (EG), a polar solvent known to improve the thermoelectric response of PEDOT:PSS.[37] After a systematic study of blend composition, film morphology, as well as mechanical and TE characterisation, a new set of materials were obtained. They are stretchable and tough, of low cost and potentially compatible with bulk industrial processing (e.g. extrusion, melt spinning), while mantaining the same Seebeck coefficient values as pure PEDOT:PSS. The sensing efficiency of these blends were then studied with the use of an

external power source, where the resistance is determined and correlated with the changes in film geometry when responding to strain. Furthermore, with a temperature difference across the end of the film, the resultant thermovoltage was found to produce a measurable sensing signal which was used to detect changes in strain as well as ambient temperature and/or air flow. The results presented in this paper promise to be a viable solution for applications such as self-powered sensors.

2. Results and Discussion

In this study, freeze-dried PEDOT:PSS and the elastomeric Lycra® yarn were separetely dispersed in dimethyl sulfoxide (DMSO), then mixed together at different proportions, aiming at maximising mechanical behaviour and strain-sensing capabilities. Free-standing films were produced by drop casting onto glass substrates. Post-treatment was performed by immersing the films in an EG bath.

2.1 – Mechanical Properties.

The mechanical properties of the blend films have been studied using quasi-static tensile tests and presented in **Figure 1a and 1b**, showing typical stress-strain responses as a function of Lycra® content. The strain-at-break value increases with increased concentration of elastomer, from $4 \pm 1\%$ at 0 wt.% Lycra® (pure PEDOT:PSS) to $300 \pm 230\%$ at 90 wt.%, while the elastic modulus is inversely correlated, going from 1300 ± 250 MPa for pure PEDOT:PSS to 23 ± 11 MPa at 90 wt.% Lycra®. Thus blending clearly improve the ductility of PEDOT:PSS. A rather large deviation in results for films with high elastomer content was observed. This is possibly due to microstructural inhomogeneities of films related to subtle variation in the casting temperature, which was demonstrated to significantly affect phase-segregation of the components (**SI-1**).

Some of the samples containing 90 wt.% Lycra® were also immersed in an EG bath after casting. They exhibited outstanding improvements in elastic modulus and strain-at-break, with values of 75 ± 65 MPa and 700 ± 150 %, respectively. These mechanical properties are unprecedented for a TE material, and closely approach the ones of neat elastomeric yarns (**SI-2**).

2.2 – Thermoelectric Properties.

A simplified way to quantify the ability of a given material to generate useful thermoelectricity, is the measurement of the power factor (PF), expressed in **Equation 1**:

$$PF = \alpha^2 \times \sigma \qquad (1)$$

where α is the Seebeck coefficient, the voltage difference generated by unit of temperature, and σ is the electrical conductivity. The power factors, electrical conductivity and Seebeck coefficient of all the blends are presented in **Figure 1c.**

The electrical conductivity of the blended films decreases linearly with increasing proportion of elastomer, from 635 ± 8 S·cm⁻¹ for unmodified PEDOT:PSS to 62 ± 4 S·cm⁻¹ for 90 wt.% Lycra®. These relatively high values can be explained by the effect of the choosen solvent (DMSO), which is known to improve the electrical conductivity of PEDOT:PSS,[55] Further improvements can be achieved if films are treated with an EG bath, giving up to 26% increase in electrical conductivity for composites containing 90 wt.% Lycra®, reaching an averaged value of 79 ± 5 S·cm⁻¹. Indeed, EG treatment consistently resulted in improved conductivity, as summarised in **SI-3**. EG has been previously shown to help controlling the film morphology through removal of excess insulating PSS.[48] The X-ray diffractograms presented in **SI-4** confirm extraction of excess PSS from the film through a reduction of signal intensity for the peak at 2θ ≈18°.

The Seebeck coefficient stayed relatively constant, invariant with the proportion of Lycra® (**Figure 1c**). This is of great importance because blends with high proportions of elastomer will

be able to produce a similar thermovoltage as neat PEDOT:PSS (useful for self-power capability), while gaining significant elasticity and toughness (as demonstrated in **Section 2.1**), Furthermore, the Seebeck coefficient of PEDOT:PSS is apparently not reduced by EG treatment (**SI-5**).

As for the electrical conductivity, also the power factor follows a similar declining trend with increasing proportion of Lycra®. Therefore, in this case, the electrical conductivity has a stronger influence than the Seebeck coefficient on PF.
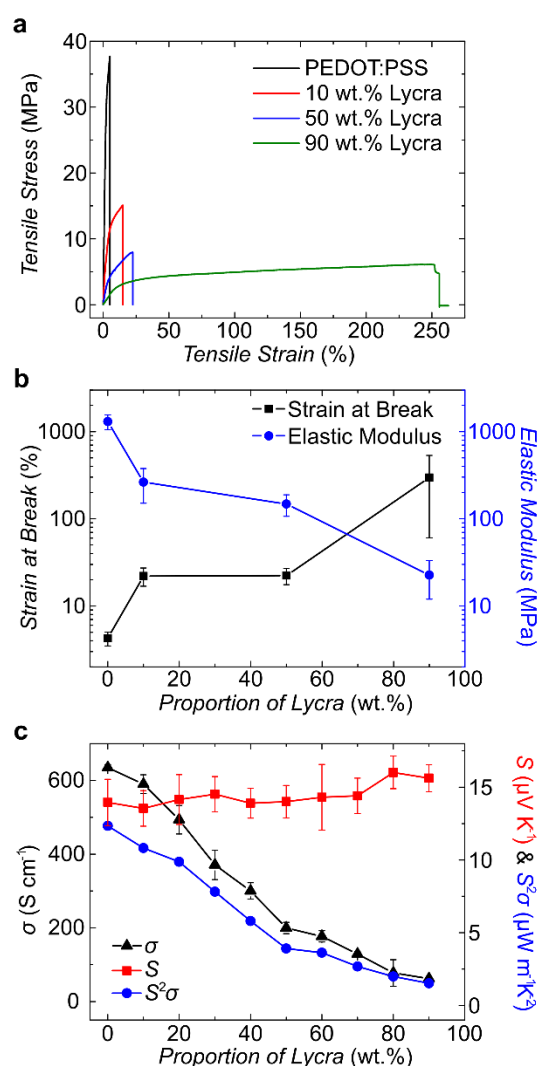

Figure 1: (a) Stress *vs* strain behaviour of PEDOT:PSS blends with various proportions of Lycra®, (b) elastic modulus and strain-at-break variations for the same blends, and (c) electrical conductivity, Seebeck coefficient and power factor of films of PEDOT:PSS blends with various proportions of Lycra® (all graphical results are before EG treatment).

2.3 – Morphology.

For a better understanding of the mechanical and thermoelectric properties presented in this paper, a systematic study of blend composition and film morphology was undertaken. Optical transmission studies of the films with varying composition revealed no evidence of a chemical reaction upon blending (**SI-6**). The study of Atomic Force Microscopy (AFM) imaging, in quantitative nanomechanical analysis mode, was used to investigate the morphology of the films, after EG treatment, shown in **Figure 2**. These images depict the relative elastic moduli of the film surfaces and clearly show the dispersion of Lycra®-rich regions (low elastic modulus) into PEDOT:PSS-rich regions (high elastic modulus), with a continuous change in the morphology between the two pure materials. Nanomechanical imaging offers in this case an improved contrast as compared to topography-mode, owing to the significant difference in elastic modulus between the two polymers. Further studies of AFM imaging revealed the Lycra®-rich regions to exhibit greater deformation, adhesion and dissipation than PEDOT:PSS-rich regions (**SI-7a**) A low degree of connectivity between domains, for films with less than 60 wt.% Lycra, is also shown in **Figure 2,** which we would expect to have detrimental effects on elasticity and toughness, as the elastomer may not be forming a continuous network, leading to more brittle and rigid materials. Yet this is not what we observed in macroscopic tests. Since these are surface images, so we cannot rule out an extended Lycra® component embedded within the film structure.

The study of topography-mode AFM imaging (**SI-7b**) revealled a root mean square (rms) roughness of 540 nm for blended films of thickness ~10 μm, which is more than an order of magnitude greater than that of commercial PEDOT:PSS cast from aqueous suspension. For the pure Lycra® films, a value of 350 nm was found.

The top surface and cross-sectional area of the blended films, before and after EG treatment, were also studied by Scanning Electron Microscopy (SEM), presented in **SI-8**. A trend toward

compact structure with increasing Lycra® content is evident, which could explain the decrease in roughness observed by AFM. No distinct microstructural differentiation is apparent in the images of films before and after EG treatment. Some isolated PEDOT:PSS domains are visible in the cross-section of films with 90 wt.% Lycra®, although the conductive pathway may not be a sole result of these apparently discontinuous sites. As previously discussed in **Section 2.1**, it is possible that the components partly phase-segregate during casting of the films.
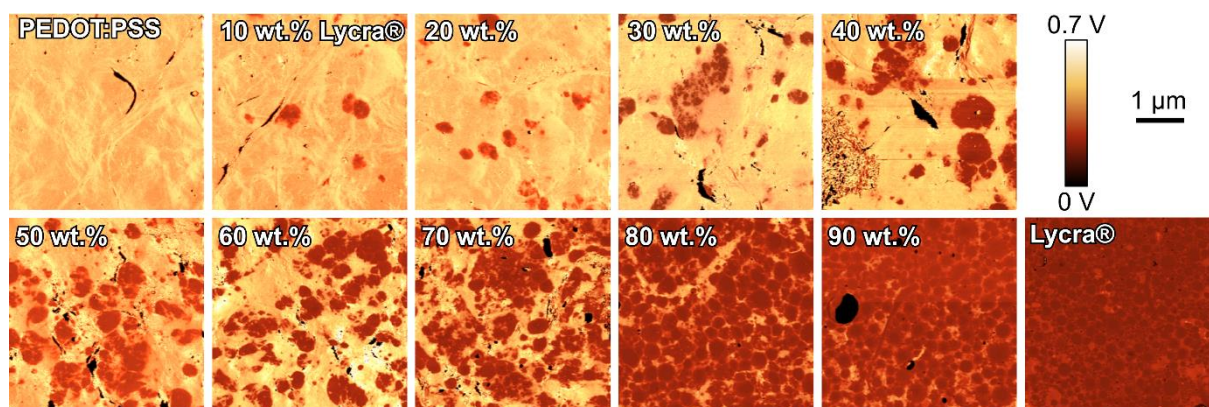

Figure 2: AFM images (4 x 4 µm) of the PEDOT:PSS/Lycra® film surfaces obtained in nanomechanical analysis mode. The colourscale is an indicator of the voltage signal from the instrument which is proportional to the elastic modulus. Lycra®-rich regions appear dark (low elastic modulus) and PEDOT:PSS-rich regions appear bright (high elastic modulus).

2.4 – Externally powered strain sensing

Sensitivity to strain was determined by a bespoke test set-up, in which the electrical resistance (R) is measured by passing a current from an external power supply through the sample while simultaneously subjecting it to a given strain profile. These tests were performed on films containing 90 wt.% Lycra®, previously subjected to EG treatment, owing to the high values of elasticity and electrical conductivity. As shown in **Figure 3a-b**, the modulation of resistance is up to 20% and 80% for strains of 10% and 50%, respectively, and this behaviour can be explained with a simple geometrical effect. By assuming incompressibility (Poisson ratio of 0.5),[56] and a constant resistivity, one can calculate the reduction of sample cross-sectional area

for a given extension, and hence a theoretical resistance (R_T), (**SI-9**). The variation of R with strain is very well predicted by this simple model. Nonetheless, for strains higher than 50%, the values of R are higher than R_T, indicating change in intrinsic resistivity may also be involved (**SI-10**). This can be explained by a possible modification of the conductive network. At relatively high strains (>80%), the sample exhibited plastic deformation, with a permanent increased resistance.

A strategy to overcome this limitation, while increasing the strain sensitivity further still, can come from engineering the conductive network morphology. It has been noticed that some samples with lower elastomer content (50 wt.% Lycra®) and prepared from poorly dissolved Lycra® presented some intact short filaments from the original yarn in the final composite film (**Figure 3c**). In these cases, the filaments indirectly control the morphology of the conductive network, in terms of excluding a volume in which PEDOT:PSS can be dispersed, but also in guiding its dispersion, which seems to preferentially coat the filaments (**Figure 3d**). Once the composite film cracks, after exceeding a threshold strain of ~10%, filaments coated with PEDOT:PSS were still observed connecting the two extremities of the cracked sample (fibre bridging), bearing the load. The strain sensing tests for these samples show an interesting bimodal behaviour. For strains lower than the threshold, the material is not sensitive, while for higher strain (after crack formation), the strain sensitivity suddenly increases (with an outstanding Gauge Factor of ~ 17,000-20,000 when 10% strain is applied). With the strain localised on the bridging filaments, it determines the pathway for charge carrier transport (**Figure 3e**). Interestingly, this change in resistance is reversible, with the normalised resistance going back to initial values before cracking, when the strain decreases to zero. In future, we envisage the development of new materials inspired by these intriguing results, where, for instance, Lycra® fibres are coated with PEDOT:PSS, which can then be used for conductive film reinforcement or as a sensing device on its own. Initial tests have already started with encouraging initial results (**SI-11**).
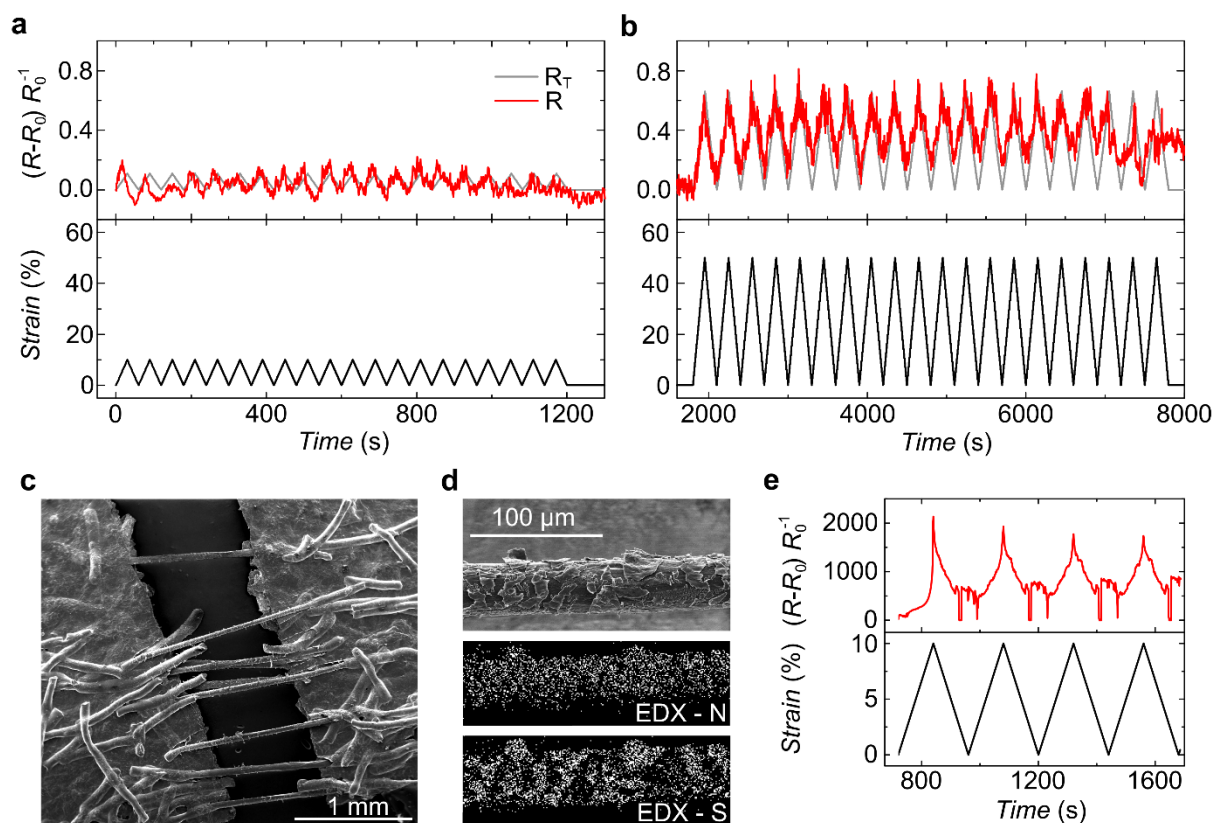
Figure 3: (a) (R-R$_0$) R$_0^{-1}$ as a function of strain, where R$_0$ is the resistance at zero strain, for films of PEDOT:PSS blended with 90 wt.% Latex® previously subject to EG treatment, when 10% strain is applied, followed by 50% (Gauge factor ~ 1 and 1.3, respectively). The theoretical resistance R$_T$ is shown in red. (b) SEM imaging of a cracked film surface of 50 wt.% Lycra® used for strain sensing, showing stretched bridging filaments, (c-d) SEM and EDX of one stretched filament for detection of sulphur (from PEDOT:PSS) and nitrogen (from Lycra®), (e) plot of (R-R$_0$) R$_0^{-1}$ as a function of strain for this film, after cracking.

2.5 – Self-powered strain sensing

To demonstrate the concept of a self-powered strain sensor based on the thermoelectric effect, a film containing 90 wt.% Lycra® was exposed to a constant temperature difference of 30 °C, while uniaxially deformed (**Figure 6a**). When the sample was series-connected to a 10 kΩ load resistor, a thermocurrent was induced by the Seebeck voltage. It is noted that the load resistance of 10 kΩ was selected to match the internal specimen resistance at high strains, hence

maximising the power output. However, the internal resistance does change with the applied strain (SI-10). So for a more efficient self-powered strain sensor, the load resistance should ideally be modulated with the strain. Nevertheless, **Figure 6c** demonstrates that large strains, above 80%, can clearly be sensed by a simultaneous change in voltage and current. In order to explain this, it is observed that the thermovoltage generated is assumed constant with strain (**SI-12**), while the resistance of the sample varies, the thermocurrent generated, passing through the external circuit also varies. Considering the equilavent circuit in **Figure 6b**, the voltage measured across the load resistor is proportional to the load resistance only, and therefore it changes proportional to the thermocurrent variation, in agreement with measurements presented in **Figure 6c**. But the self-powered sensor does not respond only to strain. In fact it shows sensitivity to other stimuli, for instance, ambient temperature and/or air currents (**SI-13**).
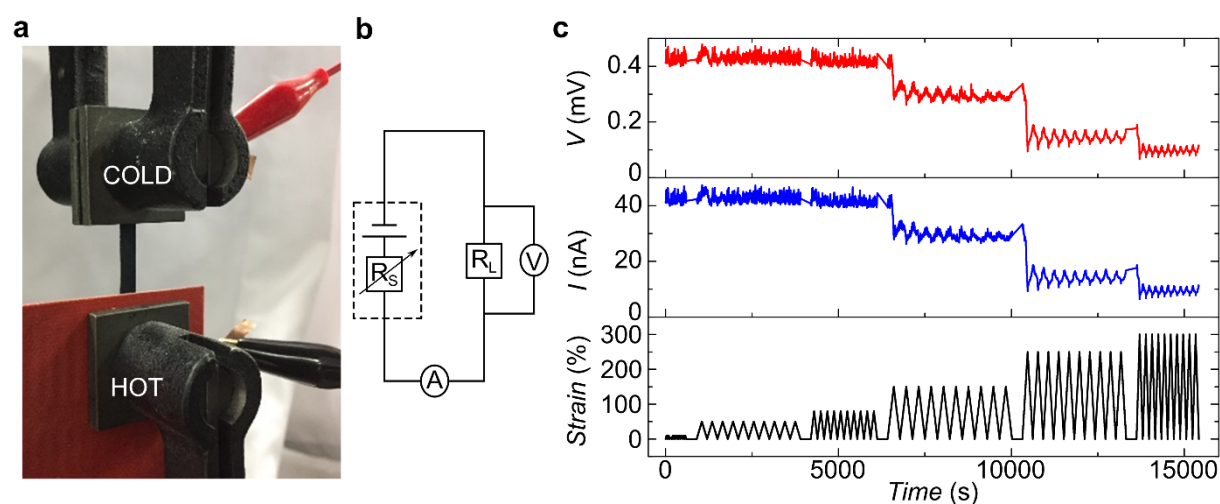

Figure 4: (a) Experimental setup for the proof-of-concept of self-powered strain sensor measurements. (b) The equivalent circuit for the film under test, the voltage source is the thermovoltage generated by the temperature difference across the ends of the sample, R_s is the internal resistance of the film and R_L is the external load resistance. (c) The variation of voltage across and current through the load resistor with strain and time.

It is noted that the sample in Figure 4, can harvest a power output of up to few nW (**SI-14**) for a ΔT of 30 °C. Increasing the power output to the level of 10-100 uW, necessary for an integrated self-powered system (including data trasmission for instance) can be achieved by: i) increasing the temperature gradient, ii) connecting our p-type TE material in series with a n-type one, to form a p-n junction, iii) connecting many p-n junctions in series.

3. Conclusion

This work demonstrates a strategy to develop stretchable self-powered sensors, via blending an elastomeric polyurethane (Lycra®) with the best organic thermoelectric material, PEDOT:PSS. In doing so, the main technological constrains of PEDOT:PSS, namely brittleness, processability and costs, have, at the same time, been overcome. An unprecedented strain at break of 700 ± 150 % has been reached, for a blend containing 90 wt.% Lycra®, after EG bath, while maintaining high electrical conductivity (79 ± 5 S·cm^{-1}) and Seebeck coefficient (16 ± 1 μV/K). This novel material has shown sensitivity to different stimuli including strain, as well as ambient temperature and/or air flow.

4. Experimental Session

PEDOT:PSS Clevios PH1000 (from Heraeous GmbH) was freeze dried (using a Benchtop Pro with Omnitronics^{TM} from SP Scientific), then dispersed in anhydrous DMSO >99.9% (from Sigma Aldrich) by homogenisation (Heidolph SilentCrusher M set at 500 rpm for 5 minutes) followed by probe sonication (Sonics VibraCell^{TM}, amplitude 35%, 1 sec on and 1 sec off, for 20 min), making up a dispersion with 1 wt.% solid content. This process could not be reproduced as efficiently if the PEDOT:PSS was dried by applying heat to the solution, which leads to a compacted dry material. On re-dispersing with DMSO, a non-homogeneous casting solution was formed, as compared to the ones using high surface area foam (**SI-15A**).

Spandex yarn (Lycra® Invista) (**SI-15B**) was also dispersed in anhydrous DMSO by stirring at 80°C for 12 hours, to afford a dispersion with 1 wt.% solid content.

Both Lycra® and PEDOT:PSS dispersions were mixed together at different proportions to make up blends of 1 wt.% load, with Lycra content varying from 0 to 100% (**SI-15C**). All mixtures were magnetically stirred for a further 24 hours at room temperature, drop cast and dried at least 10 consecutive times on pre-cleaned glass slides, using an oven set at 80ºC. Films were then mechanically removed from the glass substrate.

The drying temperature was chosen on the basis of Thermal Gravimetric Analysis (TGA) results using a TA Instruments Q500 Thermogravimetric Analyzer, flushed with air (60 ml/ min), shown in **SI-16**, with further consideration to the effect of different casting temperatures on the morphology and electrical conductivity (**SI-1**).

Mechanical tests were performed using a quasi-static tensile tester (Instron 5566, with a rate of 0.5%/ minute, then 10%/ minute for 90 wt.% Lycra blends after the first 5% strain, in this way to control the timing of the test). Films were prepared as described above, then cut at approximately 50 x 5 mm surface area. The results for % strain at break and elastic modulus were averaged out of 6 to 10 individual samples, whereas the presented curves were selected from representative results for each composition.

FTIR spectrum of solution blends were recorded using a Bruker Tensor 27, with the DMSO signal eliminated from background.

UV/Vis spectra of blends were recorded using a Perkin Elmer Lambda35. In this instance, the DMSO is not eliminated from background spectrum.

AFM images were obtained with a Bruker Dimension Icon operating in quantitative nanomechanical analysis mode on samples drop casted a single time, having films with thickness of about 10 μm.

SEM images were taken with a FEI Inspect F using FEG and EDX source. Samples were prepared by consecutively drop casted films (about 10%), with thickness of about 100 μm.

XRD signals recorded with a diffractometer system XPERT-PRO using K-alpha of 1.54Å.

A home built 4 point probe (0.25mm probe space) is used for electrical conductivity

measurements on the substrate, at room temperature and ambient atmosphere using an Agilent

6614 System DC power supply integrated with a Keithley 6485 picoammeter, connected to

the external probes. The voltage generated when current passes through the sample is then

measured (high impedance Keithley 2000 Multimeter) between the two internal probes. For

this purpose, films are prepared by single drop cast, with thickens measured using a

profilometer (Bruker Dektak Vision 64), and calculated electrical conductivity averaged out

of 4 films from each blend composition, and measured 5 times at different points within the

centre of the film.

An MMR Seebeck System was used for Seebeck measurements at 300K under nitrogen

atmosphere (SB100 digital Seebeck controller and K20 digital temperature controller), with

self-standing films cut to the dimensions required by the instrument (approximately 1 x 5 mm

surface area). The averaged result is calculated out of 3 films made from each blend

composition and measured at least 10 times each.

The electrical conductivity and Seebeck coefficient were used for calculation of the power

factor, based on **Equation 1**.

For cyclic test, as well as the self-powered strain sensing experiments, films were prepared as

described above for mechanical test. These prototype materials were then fitted with copper

electrodes on the extremities, at a distance of about 40mm apart, then padded using carbon

conductive tabs (12mm diameter from Agar Scientific), to avoid the material being pulled

from the electrode during stretching. A constant voltage of about 0.5V was applied during the

cyclic tests using an Agilent 6614 System DC power supply, while current variations with

strain recorded using a coupled Agilent 34401A 6 ½ digital multimeter. Details of theoretical

calculation model for resistance changes during the cycles were explained in **SI-9**.

For self-powered tests, heat is applied to one side of the device to generate a thermovoltage, by using a silicon heat pad (RS 12V, 7.5W, item 245-556) connected to a power supply (Farnell D30-2 set at 12V). This thermovoltage is recorded using a high impedance voltameter (Keithley 2000 Multimeter) and the current recorded using a Keithley 6485 picoammeter. Variable strain rates were used, depending on the % applied, aimed for controlling the time of test.

5. Acknowledgments

References

[1]   R. F. Service, *Science* **2003**, *301*, 909.
[2]   M. J. Cima, *Nat. Biotechnol.* **2014**, *32*, 642.
[3]   W. Zeng, L. Shu, Q. Li, S. Chen, F. Wang, X. M. Tao, *Adv. Mater.* **2014**, *26*, 5310.
[4]   A. Tricoli, N. Nasiri, S. De, *Adv. Funct. Mater.* **2017**, 1605271.
[5]   T. Dias, *Electronic Textiles: Smart Fabrics and Wearable Technology*; 2015.
[6]   About | Stanford Wearable Electronics Initiative.
[7]   S. Y. Kuang, J. Chen, X. B. Cheng, G. Zhu, Z. L. Wang, *Nano Energy* **2015**, *17*, 10.
[8]   M. Ha, J. Park, Y. Lee, H. Ko, *ACS Nano* **2015**, *9*, 3421.
[9]   H. Zhang, Y. Yang, Y. Su, J. Chen, C. Hu, Z. Wu, Y. Liu, C. Ping Wong, Y. Bando, Z. L. Wang, *Nano Energy* **2013**, *2*, 693.
[10]   Q. Shi, H. Wang, T. Wang, C. Lee, *Nano Energy* **2016**, *30*, 450.
[11]   J. Wang, S. Li, F. Yi, Y. Zi, J. Lin, X. Wang, Y. Xu, Z. L. Wang, *Nat. Commun.* **2016**, *7*, 12744.
[12]   R. Vyas, V. Lakafosis, H. Lee, G. Shaker, L. Yang, G. Orecchini, A. Traille, M. M. Tentzeris, L. Roselli, *IEEE Sens. J.* **2011**, *11*, 3139.
[13]   Y.-K. F. and H.-C. Ho, *Nanotechnology* **2016**, *27*, 95401.
[14]   N. S. Hudak, G. G. Amatucci, *J. Appl. Phys.* **2008**, *103*.

[15] A. R. M. Siddique, S. Mahmud, B. Van Heyst, *Renew. Sustain. Energy Rev.* **2017**, *73*, 730.

[16] E. A. Mondarte, V. Copa, A. Tuico, C. J. Vergara, E. Estacio, A. Salvador, A. Somintac, *Mater. Sci. Semicond. Process.* **2016**, *45*, 27.

[17] Y. Yang, Z. H. Lin, T. Hou, F. Zhang, Z. L. Wang, *Nano Res.* **2012**, *5*, 888.

[18] J. J. Kuchle, N. D. Love, *Meas. J. Int. Meas. Confed.* **2014**, *47*, 26.

[19] L. Xie, M. Cai, *IEEE Pervasive Comput.* **2014**, *13*, 42.

[20] J. Zhong, Q. Zhong, Q. Hu, N. Wu, W. Li, B. Wang, B. Hu, J. Zhou, *Adv. Funct. Mater.* **2015**, *25*, 1798.

[21] A. Dewan, S. U. Ay, M. N. Karim, H. Beyenal, *J. Power Sources* **2014**, *245*, 129.

[22] B. Sümer, E. K. San, K. Sancakdar, *Procedia Eng.* **2016**, *168*, 63.

[23] N. N. Aung, E. Crowe, X. Liu, *ISA Trans.* **2015**, *55*, 188.

[24] I. Korhonen, R. Lankinen, *Meas. J. Int. Meas. Confed.* **2014**, *58*, 241.

[25] C. Wang, K. Zhao, Q. Guo, Z. Li, *IET Circuits, Devices Syst.* **2016**, *10*, 147.

[26] V. Leonov, P. Fiorini, T. Torfs, R. Vullers, C. Van Hoof, *Proc. Int. Work. Therm. Investig. ICs Syst.* **2009**, 1.

[27] V. Leonov, T. Torfs, P. Fiorini, C. Van Hoof, *IEEE Sens. J.* **2007**, *7*, 650.

[28] S. Dalola, M. Ferrari, V. Ferrari, M. Guizzetti, D. Marioli, A. Taroni, *IEEE Trans. Instrum. Meas.* **2009**, *58*, 99.

[29] D. Davila, A. Tarancon, C. Calaza, M. Salleras, M. Fernandez-Reglez, A. San Paulo, L. Fonseca, *Nano Energy* **2012**, *1*, 812.

[30] M. Guan, K. Wang, D. Xu, W.-H. Liao, *Energy Convers. Manag.* **2017**, *138*, 30.

[31] Y. Shi, Y. Wang, Y. Deng, H. Gao, Z. Lin, W. Zhu, H. Ye, *Energy Convers. Manag.* **2014**, *80*, 110.

[32] P. J. Taroni, I. Hoces, N. Stingelin, M. Heeney, E. Bilotti, *Isr. J. Chem.* **2014**, *54*, 534.

[33] T. J. Seebeck, *Abh. Akad. Wiss.* **1822**, 289.

[34] G. J. Snyder, E. S. Toberer, *Nat. Mater.* **2008**, *7*, 105.

[35] O. Bubnova, X. Crispin, *Energy Environ. Sci.* **2012**, *5*, 9345.

[36] N. Dubey, M. Leclerc, *J. Polym. Sci. Part B Polym. Phys.* **2011**, *49*, 467.

[37] G. Kim, L. Shao, K. Zhang, K. Pipe, *Nat. Mater.* **2013**, 1.

[38] H. Julian Goldsmid, *J. Electron. Mater.* **2017**, *46*, 2599.

[39] C. Cho, K. L. Wallace, P. Tzeng, J. H. Hsu, C. Yu, J. C. Grunlan, *Adv. Energy Mater.* **2016**, *6*, 1502168.

[40] C. Cho, B. Stevens, J. H. Hsu, R. Bureau, D. A. Hagen, O. Regev, C. Yh, J. C. Grunlan, *Adv. Mater.* **2015**, *27*, 2996.

[41] C. Bounioux, P. Diaz-Chao, M. Campoy-Quiles, M. S. Martin-González, A. R. Goñi, R. Yerushalmi-Rozene, C. Müller, *Energy Environ. Sci.* **2013**, *6*, 918.

[42] B. Dörling, J. D. Ryan, J. D. Craddock, A. Sorrentino, A. El Basaty, A. Gomez, M. Garriga, E. Pereiro, J. E. Anthony, M. C. Weisenberger, A. R. Goñi, C. Müller, and M. Campoy-Quiles, *Adv. Mater.* **2016**, *28*, 2782.

[43] A. M. Nardes, M. Kemerink, R. A. J. Janssen, J. A. M. Bastiaansen, N. M. M. Kiggen, B. M. W. Langeveld, A. J. J. M. van Breemen, M. M. de Kok, *Adv. Mater.* **2007**, *19*, 1196.

[44] K.-C. Chang, M.-S. Jeng, C.-C. Yang, Y.-W. Chou, S.-K. Wu, M. A. Thomas, Y.-C. Peng, *J. Electron. Mater.* **2009**, *38*, 1182.

[45] C. Liu, B. Lu, J. Yan, J. Xu, R. Yue, Z. Zhu, S. Zhou, X. Hu, Z. Zhang, P. Chen, *Synth. Met.* **2010**, *160*, 2481.

[46] T.-C. Tsai, H.-C. Chang, C.-H. Chen, W.-T. Whang, *Org. Electron.* **2011**, *12*, 2159.

[47] A. M. Nardes, R. a. J. Janssen, M. Kemerink, *Adv. Funct. Mater.* **2008**, *18*, 865.

[48] X. Crispin, S. Marciniak, W. Osikowicz, G. Zotti, A. W. D. van Der Gon, F. Louwt, M. Fahlman, L. Groenendaal, F. De Schryver and W. R. Salaneck, *J. Polym. Sci., B,*

Polym. Phys. **2003**, 2561.

[49] O. Bubnova, M. Berggren, X. Crispin, *J. Am. Chem. Soc.* **2012**, *134*, 16456.

[50] O. Bubnova, Z. U. Khan, A. Malti, S. Braun, M. Fahlman, M. Berggren, X. Crispin, *Nat. Mater.* **2011**, *10*, 429.

[51] T. Park, C. Park, B. Kim, H. Shin, E. Kim, *Energy Environ. Sci.* **2013**, *6*, 788.

[52] T. Murakami, Y. Mori, H. Okuzaki, *Trans. Mater. Res. Soc. Japan* **2011**, *168*, 165.

[53] J. Kim, J. Jung, D. Lee, J. Joo, *Synth. Met.* **2002**, *126*, 311.

[54] F. Zhang, Y. Zang, D. Huang, C. Di, D. Zhu, *Nat. Commun.* **2015**, *6*, 8356.

[55] Q. Wei, M. Mukaida, Y. Naitoh, T. Ishida, *Adv. Mater.* **2013**, *25*, 2831.

[56] H. J. Qi, M. C. Boyce, **2004**, 1.